



Full length article

## Development and evaluation of empagliflozin-loaded solid lipid nanoparticles: Pharmacokinetics and pharmacodynamics for oral delivery

Ananda Kumar Chettupalli<sup>a,\*</sup>, Aziz Unnisa<sup>b</sup>, Himabindu Peddapalli<sup>c</sup>, Rajendra Kumar Jadi<sup>c</sup>, Kachupally Anusha<sup>c</sup>, Padmanabha Rao Amarachinta<sup>c</sup>

<sup>a</sup> Department of Pharmaceutical Sciences, Center for Nanomedicine, School of Medical and Allied Sciences, Galgotias University, 201310, Greater Noida, Uttar Pradesh, India

<sup>b</sup> Department of Pharmaceutical Chemistry, College of Pharmacy, University of Hail, Hail, K.S.A, India

<sup>c</sup> Department of Pharmaceutics, School of Pharmacy, Anurag University, Venkatapur, Ghatkesar, Medchal-Malkajgiri, Hyderabad, Telangana - 500 088, India

## ARTICLE INFO

## Keywords:

Solid lipid nanoparticles  
Pharmacokinetics  
Bioavailability  
Homogenization  
Central composite design  
Oral formulation

## ABSTRACT

Type 2 diabetes mellitus is frequently treated with empagliflozin (EZN), a sodium-glucose cotransporter 2 inhibitor. Solid lipid nanoparticles (SLNs) shield the drug from gastrointestinal breakdown and improve the bioavailability of lipophilic drugs. The aim of the study is to use SLNs to enhance EZN's pharmacokinetics and pharmacodynamics in the treatment of diabetes mellitus. To prepare EZN-loaded SLNs, central composite design (CCD) was employed. The optimized batch (optimized EZN-loaded SLNs) had the desired values of dependent variables Vesicle size (R1), Entrapment Efficiency (R2), and Cumulative Drug Release (CDR) (R3). This was achieved by using analysis of variance (ANOVA) to analyse independent variables such as lipid concentration (X1), surfactant concentration (X2), sonication time (X3), and homogenization speed (X4). F8 exhibited the highest drug entrapment ( $90.6\% \pm 2.8\%$ ), CDR ( $89.2 \pm 3.6$ ), and average particle size ( $98.6 \pm 2.1$  nm) among the 30 distinct formulated formulae (F1–F30). Based on the F-value and p-value, the model was determined to be significant for particle size, entrapment efficiency, and CDR. The actual values of particle size entrapment efficiency and CDR closely matched the projected values of the optimized batch. The in vitro release trials produced a burst release followed by a continuous release. When compared to the EZN solution, the relative bioavailability of EZN-loaded SLNs was 1.2 times higher, indicating superior protection against the gastrointestinal environment. In rats with streptozotocin-induced diabetes mellitus, the optimized EZN-loaded SLNs outperformed the basic drug suspension in terms of antidiabetic efficacy. One promising method for administering EZN in the treatment of diabetes mellitus is by SLNs.

## 1. Introduction

Metabolic and chronic, Diabetes Mellitus (DM) causes elevated blood sugar levels owing to insufficient insulin synthesis or insulin action, or both. The current global prevalence of DM is 425 million, with an expected increase to 642 million by the year 2040. Among the several oral anti-diabetic medications available for the treatment of diabetes are sulfonylureas, biguanides, alpha-glucosidase inhibitors, meglitinide analogues, and thiazolidinediones. Metformin, alpha-glucosidase inhibitors, sulfonylureas, and insulin are just a few examples of medications that might cause hypoglycemia and weight gain, or gastrointestinal side effects. The prevalence of type 2 diabetes mellitus (T2DM), which rises as a result of obesity, genetic predisposition, and other

lifestyle diseases, is disproportionately high in the senior population (around 95%). At now, a lot of diabetic medications are utilized to control type 2 diabetes. The process involves halting glucose reabsorption from Henley's loop, increasing insulin synthesis, and decreasing insulin resistance. Pharmacists mostly focus on diabetes management.<sup>1–4</sup>

Empagliflozin (EZN) is a Some nanoparticle formulations (such liposomes, which are vesicular structures) share comparable size ranges Class III drug used to manage DM. Empagliflozin has a high solubility in gastrointestinal fluids, making it a BCS Class III medication. Intestinal mucosa is one example of a biological membrane with low permeability. The medicine has a high solubility, which means it dissolves rapidly in the digestive tract, but its low permeability means that only a tiny amount of it can enter the bloodstream, even though it dissolves easily. In

\* Corresponding author.

E-mail address: [anandphd88@gmail.com](mailto:anandphd88@gmail.com) (A.K. Chettupalli).

<https://doi.org/10.1016/j.ipha.2024.12.004>

Received 12 October 2024; Received in revised form 21 December 2024; Accepted 24 December 2024

Available online 12 January 2025

2949-866X/© 2025 The Authors. Publishing services by Elsevier B.V. on behalf of Higher Education Press and KeAi Communications Co. Ltd. This is an open access article under the CC BY license (<http://creativecommons.org/licenses/by/4.0/>).

most cases, improving permeability is more important than increasing solubility for BCS Class III medicines. Even though Empagliflozin has enough solubility, its limited permeability and poor absorption can nevertheless reduce its therapeutic efficacy and oral bioavailability. One possible solution in this case is the use of solid lipid nanoparticles, or SLNs. With a size typically in the nanometre range, SLNs are incredibly microscopic. Due to factors such as increased uptake by enterocytes (intestinal cells), lymphatic transport, or endocytosis, this diminutive size can improve intestinal absorption, resulting in improved bioavailability. A solid lipid core is the main component of SLNs and can store the drug, which could enable regulated or sustained release. The drug's total systemic circulation exposure can be enhanced in this way. When administered with SLNs, drugs have a better chance of penetrating cell membranes via the lipid bilayers. To improve absorption, lipid nanoparticles can interact with specific transporters or modify the shape of intestinal cell membranes. The study's main objective is to assess the inhibition of sodium-glucose cotransporter (SGLT2) in people with diabetes while enhancing solubility and bioavailability.<sup>5</sup> A medicine that inhibits SGLT and is used to treat diabetes is EZN, which is also called 1, 5-anhydro-1-(4-chloro-3-tetrahydrofuran-3-yloxy) D-Glucitol. It reduces blood sugar levels and cures type 2 diabetes by blocking SGLT-2 and making glucose be removed through urine. Newer molecules for the treatment of diabetes include anti-diabetic medicines that work by directing the kidneys to excrete glucose.<sup>6,7</sup> Metabolic changes, gastric issues, weight gain, fluid retention, hypoglycemia, and other well-documented adverse effects.<sup>7,8</sup> As a result of its efficacy and safety in managing glucose, EZN has become a prominent medication option on a global scale. In most cases, taking 10 mg orally each day, with or without food, has no ill effects and is easily absorbed. To enhance the hypoglycemic effects of other hypoglycemic drugs, they can be given together.<sup>6,9,10</sup>

Lipid-based solid lipid nanoparticles (SLNs) offer several gains, such as the ability to include hydrophobic/lipophilic medicines, targeted drug delivery, elimination of organic solvents, favorable acceptableness, stability, and viability for large-scale production.<sup>11,12</sup> SLNs are at the forefront of the rapidly emerging field of nanotechnology.<sup>8,10,13</sup>

Researchers have investigated lipid-based nanoformulations to enhance poorly soluble drugs' solubility, dissolution, and absorption profile.<sup>14–17</sup> The usage of lipid systems is crucial since it is expected to boost oral absorption in a similar manner to the lipid components of a typical diet.<sup>18</sup> Harde et al have explained the mechanistic method of SLNs absorption via the oral route in detail.<sup>19</sup> SLNs of 50–1000 nm, typically unaltered, have demonstrated sufficient particle absorption via the lymphatic route.<sup>20</sup> Additionally, SLNs have been transported to numerous organs of the body's lymphatic systems in particulate form by the colon via an intracellular or paracellular route.<sup>15,16,19</sup>

In addition to their nano size and unique structural features, the SLNs exhibit high drug-loading capacity and biocompatibility.<sup>13,21</sup> It consists of a lipid core en-cased in a lipophilic drug and an outer shell with a surfactant.<sup>15</sup> Which intern improves intestinal permeability and absorption. It keeps drugs from degrading in an acidic environment and enhances their absorption into the bloodstream.<sup>17</sup> SLNs avoid the usage of the protein complex P-glycoprotein (P-gp) and first-pass metabolism by the aid in transporting the drug to the lymphatic system. They also help in intestinal permeability and drug absorption. Drug absorption in the systemic circulation is improved by SLNs, which protect against drug breakdown in an acidic environment.<sup>22</sup>

CCD design is a cutting-edge method for formulation optimization since it requires fewer trials and less time. The response surfaces methodology aims to comprehend how fundamental aspects affect the response and arrive at optimal for-mulations with predetermined objectives.<sup>23,24,25,26,27</sup> RSM (Response Surface Methodology) reduces the number of tests while still allowing for a thorough investigation into the effects of several variables. Applying RSM's statistical and mathematical methodolo-gies, one may achieve process development, improvement, and optimization.

The study aimed to find the best conditions for loading SLNs with EZN utilizing a CCD design. Mean particle size and EE were evaluated as well as PDI and zeta poten-tial as a reaction to factors such as lipid content, surfactant concentration, and homogenization speed. The potential formulation will be subjected to various studies such as solid-state characterization, surface morphology, drug release kinetics, and in vitro and in vivo confirmative studies.

## 2. Materials and methods

Hetero Pharma (Pvt.) Ltd. Hyderabad generously contributed EZN (API) as a gift sample for the study. The materials such as standard, lupeol (95% purity), poloxamer 188 (Pluronic F-68), and palmitic acid (melting point, 69.3 °C; mol. weight, 284.5 g/mol) were procured from Sigma–Aldrich Chemicals Pvt. Ltd., Bangalore, India. Glyceryl monostearate, Tween 80, and sodium deoxycholate were purchased from Hospira Healthcare India Pvt. Ltd., Chennai, India. Dialysis membrane (MW 12,000–14,000 Da) procured from Hi–Media, India. Milli-Q plus water was used in all tests (Millipore, India).

### 2.1. Preliminary screening

#### 2.1.1. Selection of solid lipid

Palmitic acid, cetyl alcohol, and glyceryl monostearate were used to study the solubility of EZN. Since EZN is lipid-soluble, it was selected for developing SLNs. An accurate or precise quantity of the EZN drug was blended with molten lipids as well as warm distilled water. After that, it was shaken for 45 min over a hot water bath to measure the solubility factor. Under constant stirring and heating, gradually add the lipid to the solution until clear, homogenous liquid results. Total EZN solubility was calculated for each lipid.<sup>22–28</sup>

#### 2.1.2. Selection of surfactant

The preparation method of optimized SLNs may influence the choice of surfactant. The nanoparticles' size and degree of polydispersity are directly affected by the con-centration and quantity of surfactant utilized to manufacture the suspension of SLNs. A volume of 1 mL of surfactant solution, was added to an Eppendorf tube together with Tween 20, Tween 80, PEG200, Limonene, and Cremophor EL. Subsequently, the surplus EZN and the tube were subjected to agitation for a duration of 15 min. The solution was allowed to incubate for a duration of 72 h using an orbital shaker. Following centrifugation of the mixture at a speed of 5000 revolutions per minute for a duration of 15 min, the supernatant was subsequently gathered and subjected to separation. The quantification of EZN was conducted at a wavelength of 224 nm using a spectrophotometer, following appropriate dilution procedures.<sup>22</sup>

#### 2.1.3. Selection of stabilizer

The titration approach was used to determine the best stabilizer for the experi-ment's needs. Lecithin, glycerol behenate, poloxamer 188, and a (synthetic stabilizer) Labrasol VR were investigated. At 65 °C, a uniform solid lipid mixture was heated with various co-surfactant combinations (at different weight-to-weight ratios). Drop by drop, under constant stirring, the resultant combinations were gradually titrated until they became cloudy. A dispersion percent range was obtained for each stabilizer capable of dispersion.<sup>29</sup>

#### 2.1.4. Selection of sonication time and amplitude

Based on its superior repeatability and high intensity, probe sonication was chosen. The reduction in particle size can be achieved by raising the intensity of ultrasonic waves and prolonging the duration of sonication. Nevertheless, once beyond a specific threshold, the augmentation of both the period and amplitude leads to an escalation in the size of particles due to the phenomenon of particle aggregation. The optimal amplitude and duration of sonication were discovered through rigorous experimentation. A stabilizer and surfac-tant were used to make

the SLNs. For about 5–8 min, formulations were sonicated at 20%, 40%, and 50% amplitudes and were assessed for entrapment effectiveness and particle size.

## 2.2. Preparation of SLNs from EZN

The method of hot homogenization, followed by ultrasonication, was employed in the preparation of EZN-SLNs. A predetermined quantity of EZN, Lipid, and poloxamer 188, Specifically, 10 mg was dissolved in a predetermined volume of ethanol and then heated in a water bath to 75 °C. This process facilitated the formation of a lipophilic phase. Simultaneously, to produce an aqueous phase, a precise quantity of Tween-80 was dissolved in a suitable volume of distilled water and heated to the same temperatures as the lipid phase. The lipid phase was combined with the aqueous phase under magnetic stirring and afterwards homogenized at a speed of 15,000 rpm for a duration of 10 min producing a suspension with a high-speed Ultra Turrax T25 homogenizer (IKA®Labortechnik, Germany). The suspension underwent ultrasonication using an ultrasonic cell crusher (Sonics, USA) operating at a power of 300 W for a duration of 5 min. Following this, the suspension was subjected to centrifugation at a temperature of 4° or a 30-min window in order to extract it EZN-loaded solid lipid nanoparticles (SLNs). The emulsion system created, known as EZN-SLNs, was thereafter kept at a temperature of 4 °C. The EZN solid lipid nanoparticles (SLNs) were subjected to additional characterization using Fourier-transform infrared spectroscopy (FTIR), differential scanning calorimetry (DSC), and X-ray diffraction (XRD) techniques.<sup>25</sup>

## 2.3. Factorial research design

EZN-SLNs formulations were designed by identifying the factors that may impact the intended formulation attributes.<sup>26</sup> Using a CCD and Design Expert® software (DoE) could improve the performance of SLNs (12.0.3.0, Stat-Ease Inc., Minneapolis, 11 MN, USA). The independent variables, such as lipid concentration (X1), surfactant concentration (X2), sonication time (X3), and homogenization speed (X4), were all considered. The dependent variables used were Vesicle size (R1), Entrapment Efficiency (R2), and cumulative drug release (CDR) (R3) were optimized to get the best values for each parameter. The program created a total of 30 runs (Table 1). The PDI, zeta potential, and mean particle size of the SLNs were all expressed using second-order polynomial equation (28).

The following is the polynomial equation that was derived from the experiment:

$$Y_i = b_0 + b_1X_1 + b_2X_2 + b_3X_3 + b_{12} \times 1 \times 2 + b_{13} \times 1 \times 3 + b_{23} \times 2 \times 3 + b_{112}X_{12} + b_{222}X_{22} + b_{333}X_{32}$$

There is a correlation between each component level combination and the re-sponse of the dependent variable, which is described in terms of particle size, EE, CDR, and b0 an intercept. The correlation between the factors and the outcomes was evaluated using the *P*-values associated with the regression coefficients. The model's appropriateness was assessed using an analysis of variance and a predicted *R*<sup>2</sup> value.<sup>30</sup>

**Table 1**  
Formulation variables of EZN SLNs.

Parameter	Low (−1)	Medium (0)	High (+1)
Independent Variables			
Lipid Concentration (X1)	2	5	8
Surfactant (X2)	1	1.75	2.5
Sonication Time (X3)	2.5	5	7.5
Homogenization Speed (X4)	5000	7500	10000
Dependent variables			
R1: Vesicle Size (nm)	Maximize		
R2: Entrapment Efficiency (%)	Minimize		
R3: Cumulative Drug Release (%)	Maximize		

## 2.4. Statistical analysis

The influence of the formulation variables was examined using ANOVA and how they interact with the outcomes. Following *p*-values, adjusted *R*<sup>2</sup> and predicted *R*<sup>2</sup> were employed to select the best-fit model using the DoE program. The significance of each factor is indicated by a *p* ≤ 0.05 and an *F*-value >0.05.<sup>31</sup> 3D surface plots and counterplots were made using DoE software to illustrate the relationship between the independent factors and dependent variables. A negative sign on a coefficient's magnitude indicates an antagonistic impact on responses.

## 2.5. Optimized formulation

SLNs loaded with EZN were chosen for their high EE, high zeta potential, and tiny particle size as the optimal formulation. The overlay plot was created using a graphical optimization approach depending on the desired function between 0 and 1. SLNs were built using the predicted values with the most excellent desirability function (R1-0.9748, R2-0.9581, and R3-0.9695) to acquire the actual values.<sup>32</sup> The results of the experiments were compared to the predicted values.

## 2.6. Characteristics of SLNs

### 2.6.1. Size, PDI, and zeta potential of particles

SLNs formulations' particle size, PDI, and zeta potential were evaluated using dynamic light scattering. The samples were analyzed for particle size and PDI analysis, recorded at a constant angle of 165° and a temperature of 25 °C. Triplicate readings of the PDI and Zeta potential were taken. (*n* = 3). Particle size was calculated using the Stokes–Einstein relation.<sup>33</sup> The Zetasizer Nano ZS90 has been used to quantify the zeta potential (ζ) of EZN-SLNs. The electrophoretic mobility of the particles is converted into zeta potential using Henry's equation: (μ):

$$\mu = 2\zeta\epsilon/3\eta_0 f(Kr)$$

Particle radius to Debye double-layer thickness ratio *Kr* is (i.e., water viscosity). Henry's function is referred to as *f* (*Kr*). A total of three times each measurement was recorded.

### 2.6.2. Drug loading and entrapment efficiency (% EE)

SLNs were centrifuged in the supernatant for 30 min at 10,000 rpm (REMI laboratory Instrument, Mumbai, India) to remove the pellet to assess the efficacy of EZN. UV spectroscopy (UV1800, Shimadzu, Japan) was used to determine the quantity of free EZN in the supernatant. Using a standard curve for absorption and a known concentration of EZN, we could determine how much EZN was free in the supernatant. % EE was calculated using an aqueous surfactant solution. Separation was accomplished by centrifuging the water from the rest of the sample. The dispersion of EZN-SLNs was centrifuged in Eppendorf tubes for 30 min at 10,000 rpm and 4 ± 1 °C. EZN was quantified in the supernatant by using UV-spectrophotometric analysis.<sup>34</sup> The calibration curve was used to measure the EZN concentration, and the following equation was used to compute the % EE:

$$\text{Entrapment Efficiency (\%)} = (\text{Amount of drug in formulation} - \text{Amount of the drug in supernatant}) / (\text{Amount of the drug in the formulation})$$

$$\text{Drug Loading (\%)} = (\text{Amount of drug in formulation} - \text{Amount of the drug in supernatant}) / (\text{Amount of drug in formulation} + \text{polymer weight})$$

### 2.6.3. Drug content

The drug concentration was determined by dilution with 10 mL of methanol of 0.1 mL of SLNs. The solution was siphoned into a syringe and sonicated for 2 min, finally separated using a Millipore filter paper (0.045-μm).<sup>35</sup> The solution's chemical composition was determined using

a spectrophotometer at 224 nm. The formula was used to determine the amount of drugs present.

Drug Content (%) = (Amount of drug)/(obtained, total drug added) X100

#### 2.6.4. Morphological studies

**2.6.4.1. Scanning electron microscopy (SEM).** SEM examined the SLNs' particle size and shape (Model: Hitachi S3400, Tokyo, Japan). Primary and secondary electron emission SEM was used to investigate how the SLNs samples behaved in their native environment. Then the morphology of these samples was studied at a 15 kV acceleration voltage scan.<sup>36</sup>

**2.6.4.2. Atomic force microscopy (AFM).** AFM was used to examine the surface characteristics of SLNs loaded with EZN (NT-MDT Solver NEXT, Russia). AFM was used to investigate an aqueous nanosuspension layer formed on a clean microscope slide.<sup>37</sup>

**2.6.4.3. Transmission electron microscopy (TEM).** A transmission electron microscope (TEM) was employed to examine the morphological characteristics of the sentinel lymph nodes (SLNs). A minute quantity of EZN-SLNs was applied onto the carbon-coated copper grid, followed by the addition of phosphotungstic acid (2% v/v) to facilitate sample staining. The specimen was subjected to a 10-min incubation period, after which any surplus material was eliminated using filter paper. The sample, which had been stained and dried, was carefully placed in the electron microscope apparatus to facilitate examination. Subsequently, the electron microscope was employed to take an image of the sample, which was subsequently subjected to detailed analysis.<sup>38</sup>

#### 2.7. In vitro release study

EZN solubility tests were performed using a UV–visible spectrophotometer, it was submerged for 2 h at pH 1.2, then transferred for 2 h to pH 6.8, and finally to pH 7.4. The sink condition for EZN dissolution was achieved in vitro tests using a SIF pH 7.4 solution. 1% solution of Tween 80 in SIF phosphate buffer pH 7.4, and the study was carried out in accordance with ICH recommendations. The study uses a diffusion method through which the particle permeated in vitro drug release studies. Prior to conducting the experiment, distilled water was pre-soaked in the dialysis membrane (molecular weight cut-off: 12–14 kDa), which was then filled with 10 mg of the drug solution and optimized EZN-SLNs. The dialysis membrane tube was sealed at both ends once it had been filled. SIF and phosphate buffer 7.4 were used to store the dialysis tube. At a temperature of  $37 \pm 1$  °C, samples were shaken and centrifuged at 100 rpm. A 1 mL sample was obtained at a specific interval and examined using a UV spectrophotometer. When the level was at that removed and refilled nearly, it maintained the sink state conditions ( $n = 3$ ). The investigation of drug release kinetics from solid lipid nanoparticles (SLNs) was conducted through the utilization of various numerical models, namely the Higuchi model, the Korsmeyer-Peppas model, and the zero-order kinetics model. The graphical representation illustrates the progressive accumulation of drug quantities discharged over a period of time.<sup>39</sup> The percentage of cumulative data reduction (CDR) against the square root of time was plotted. The Korsmeyer-Peppas model is employed to elucidate the diffusion behavior of both Fickian and non-Fickian processes, with the coefficient's magnitude serving as a means of determination. The release kinetics of a drug were analyzed by plotting the logarithm of the cumulative drug release percentage (% CDR) against the logarithm of the time, using data obtained from in vitro drug release studies.

#### 2.8. Characterization of solid states

##### 2.8.1. FTIR studies

FIR spectroscopy was used to study the interaction between EZN and excipients (FTIR-8400S, Shimadzu). Using the standard KBR pellet technique, the FTIR spectra of EZN, Palmitic acid, and SLNs were obtained. Anhydrous KBr powder was used for crushing and compressing the samples into pellets. For a total of 50 scans, With a resolution of  $4 \text{ cm}^{-1}$ , FTIR spectra between 4000 and  $400 \text{ cm}^{-1}$  were collected.

##### 2.8.2. DSC

For Obtaining the DSC, thermograms of the samples EZN, Palmitic acid, and SLNs were studied using a DSC (DSC25, Mettler Toledo, USA). Samples were weighed and scanned in an aluminum pan at 30–300 °C in a dry nitrogen environment. The interaction between drugs and lipids was studied using thermograms and at a heating rate of 5 °C/min.<sup>40</sup>

##### 2.8.3. X-ray diffraction studies

The degree of crystallinity of the samples EZN, Lipid, Surfactant, and Optimized SLNs can be tested with an X-ray diffractometer. The physical properties of EZN, lipoprotein (palmitic acid), drug, and lipoprotein were analyzed using X-ray patterns obtained using a diffractometer (Rigaku, Smart lab) under Cu Ka radiation as the X-ray source at a voltage of 45 kV and an applied current of 80 mA(42).

#### 2.9. Pharmacokinetic studies

Pharmacokinetic studies were performed at Nalanda College of Pharmacy, Nalgonda (proposal number IAEC/NCP/2022-006), with animal experiments performed in a recognized animal house facility. The Sprague Dawley rats used in the experiments weighed between 180 and 220 g and were approximately six weeks old when they were obtained from the National Institute of Nutrition in Hyderabad. The in vivo bioavailability tests were performed on 12 rats, and they were randomly assigned to one of two treatment groups. Group A was given EZN (pure drug), while Group B received Optimized SLNs. Prior to the experiment, the animals were starved for the whole night, although they were given unrestricted access to water. Each group of rats received orally administered capsules containing SLNs and EZN at 10 mg/kg of body weight. For investigations, 0.5 mL of blood was withdrawn into a microcentrifuge tube at 0, 2, 4, 8, 12, 24, 36, and 48 h using the retroorbital plexus technique. After collecting the samples, they were centrifuged for 20 min at 5000 g. After collection, the plasma was kept at 20 °C for future analysis. By combining 180 mL of plasma with 1.8 mL of dichloromethane in a vortex for 3 min, the plasma was deproteinized. The organic supernatant was transferred to a clean tube after being centrifuged at 10,000 rpm for 10 min at 4 °C. A gentle stream of nitrogen was then used to dry the organic supernatant. The residue was reconstituted and mixed in a vortex mixture using a 120 µL mobile phase consisting of methanol: acetonitrile (75:25) and a 10 µL EZN (10 mg/mL) internal standard was used. After centrifuging the suspension at 10,000 rpm for 10 min, A 20 µL portion of the supernatant was added to the HPLC for recording. the chromatograms at 222 nm. The chromatographic column was maintained as per the protocol. The flow rate and wavelength were adjusted slightly for the in vitro analysis. Parameters of pharmacokinetics were determined using the non-compartmental assay (NCA) module of the WinNonlin® 6.1 pharmacokinetic software program.

#### 2.10. Pharmacodynamic study

##### 2.10.1. Animals

The Animals were purchased from the National Institute of Nutrition's

albino Sprague Dawley (SD) rats weighing 200–250 g. (Hyderabad, India). The IAEC of the School of Pharmacy, Nalanda College of Pharmacy, Hyderabad, Telangana (reference number IAEC/NCP/2022-006) authorized all animal research. At a constant temperature of  $22 \pm 2$  °C, four animals were housed in independent cages. All of the animals were given unlimited access to food and water. (Golden Feeds, New Delhi). Dark and light cycle studies were performed.<sup>41</sup>

### 2.10.2. Induction of diabetes

Streptozotocin (STZ) was injected intraperitoneally into SD rats at 60 mg/kg body weight to develop diabetes. The citrate buffer in which the STZ was dissolved was ice-cold. To combat the hypoglycemia caused by STZ, the animals were given a 5% glucose solution to consume throughout the night. A diabetic animal was defined as having a blood glucose level higher than the standard value after receiving an STZ injection for three days. A blood glucose level of 200 mg/dL was attained after inducing STZ. On the fourth day following the STZ injection, treatment was initiated, and it lasted for a total of 28 days. After the experiment, blood glucose and body weight were monitored and measured on days 0, 7, 14, 21, and 28(44).

### 2.10.3. Experimentation

Randomly, six animals were placed in each group. STZ was administered to groups II, III, and IV to induce diabetes, whereas group I remained nondiabetic. As a diabetic control, group II got blank SLNs, while the third group (100 mg/kg p.o.) got the pure drug solution (by oral route). Group 4 got the most improved EZN-SLNs (100 mg/kg p.o.), while group I received blank SLNs (5 mg/kg p.o.).

### 2.10.4. Accelerated stability studies

The stability studies were conducted as per the methods provided by Chalikwar and the ICH Q1A(R2) guidelines in conjunction with the optimized batch of EZN-SLNs for stability experiments.<sup>42,43</sup> The dosage forms were kept in a refrigerator at 5 °C and 25 °C/60% RH, respectively, while conducting long-term stability and accelerated stability testing, in accordance with ICH standards. To investigate the particle

size, EE, and CDR stability of SLNs, a 24-h accelerated stability research at 25 °C/60% relative humidity was performed. The samples were stored for six months under dry conditions. Later, the SLNs were prepared freshly and studied for their stability behavior (the CHM-10S from Remi Instruments Ltd., Mumbai, India). The samples were reconstituted in deionized water and analyzed for particle size, EE %, and CDR percentage every month.<sup>44</sup>

### 2.10.5. Statistical analysis

The data is provided as three independent replications ( $n = 3$ ) of mean and standard deviation. The data were subjected to analysis using GraphPad Prism Software, developed by GraphPad Software Inc. in San Diego, California, United States. The determination of significance values in Using one-way ANOVA and Tukey–Kramer multiple comparisons testing, this study was carried out. The threshold for statistical significance is commonly set at a significance level of 0.05.

## 3. Results & discussion

### 3.1. EZN solubility studies in different lipids

Evaluation of solubility in Glyceryl monostearate, cetyl alcohol, and Palmitic acid was used to select the suitable lipid for the formulation. Glyceryl monostearate, Cetyl Alcohol, and palmitic acid had concentrations of  $0.39 \pm 0.17$  mg/mL,  $0.26 \pm 0.14$  mg/mL, and  $0.56 \pm 0.42$  mg/mL, respectively. Out of the lipids described above, palmitic acid was more soluble, so it was selected for making SLNs.

### 3.2. Selection of stabilizer

Out of the four stabilizers, poloxamer 188 has shown high entrapment efficiency and small particle size compared to other stabilizers studied; it is possible to make SLNs with or without stabilizers. Table 2 shows how the stabilizers of SLNs impact the preparation. As a result, a 1% stabilizer was added to all the formulations to improve their quality. Table 3 displays the optimal particle size for entrapping the maximum number of particles.

**Table 2**

The make-up of the 30 runs produced by CCD and the observed results.

Run	X1	X2	X3	X4	R1	R2	R3	Zeta	PDI
1	5	1.75	5	7500	306 ± 3.6	60.3 ± 2.1	55.6 ± 0.5	-15.6 ± 1.2	0.195 ± 0.01
2	8	2.5	2.5	5000	426 ± 7.4	53.8 ± 3.5	65.3 ± 3.2	-18.3 ± 0.6	0.286 ± 0.01
3	2	2.5	7.5	10000	431 ± 4.2	50.9 ± 3.3	60.2 ± 1.2	-20.4 ± 0.9	0.316 ± 0.02
4	5	1.75	0	7500	395 ± 1.9	62.8 ± 1.2	57.3 ± 1.5	-23.4 ± 0.5	0.246 ± 0.05
5	8	1	2.5	5000	412 ± 3.5	50.6 ± 1.6	47.5 ± 2.3	-21.6 ± 0.3	0.198 ± 0.02
6	2	2.5	7.5	5000	426 ± 2.7	53.7 ± 1.4	57.9 ± 0.9	-17.9 ± 0.4	0.264 ± 0.04
7	5	1.75	5	2500	286 ± 6.5	68.2 ± 2.1	74.2 ± 1.0	-26.5 ± 0.1	0.352 ± 0.02
8	8	2.5	2.5	10000	98.6 ± 2.1	90.6 ± 2.8	89.2 ± 3.6	-35.6 ± 1.2	0.023 ± 0.03
9	2	1	2.5	5000	412 ± 3.5	48.2 ± 3.2	45.9 ± 2.5	-28.4 ± 1.1	0.325 ± 0.02
10	8	1	7.5	10000	296 ± 6.4	72.9 ± 3.1	69.5 ± 2.4	-26.4 ± 0.9	0.126 ± 0.01
11	11	1.75	5	7500	354 ± 1.6	60.5 ± 1.1	65.3 ± 1.2	-22.1 ± 0.2	0.218 ± 0.02
12	5	1.75	5	12500	261 ± 5.2	80.3 ± 1.8	79.2 ± 2.1	-26.4 ± 0.1	0.135 ± 0.04
13	5	3.25	5	7500	328 ± 3.9	74.5 ± 1.3	69.5 ± 3.2	-23.9 ± 0.2	0.267 ± 0.02
14	2	2.5	2.5	10000	323 ± 2.8	69.2 ± 2.5	64.3 ± 2.3	-14.2 ± 0.4	0.098 ± 0.06
15	5	1.75	5	7500	335 ± 3.1	60.3 ± 1.6	55.6 ± 1.1	-19.1 ± 0.2	0.265 ± 0.02
16	2	1	7.5	10000	356 ± 3.8	75.8 ± 3.2	79.1 ± 1.2	-23.4 ± 0.6	0.098 ± 0.05
17	5	1.75	5	7500	331 ± 2.4	60.3 ± 4.2	55.3 ± 1.3	-30.5 ± 1.3	0.254 ± 0.02
18	2	1	2.5	10000	321 ± 2.9	75.2 ± 3.1	65.4 ± 3.5	-25.4 ± 0.5	0.394 ± 0.01
19	5	1.75	5	7500	338 ± 3.2	60.3 ± 1.6	54.3 ± 4.2	-29.8 ± 0.4	0.526 ± 0.23
20	5	1.75	5	7500	334 ± 3.5	60.3 ± 2.5	55.1 ± 0.8	-29.7 ± 0.3	0.642 ± 0.11
21	5	1.75	10	7500	226 ± 2.6	68.4 ± 2.7	73.5 ± 0.5	-30.5 ± 0.5	0.597 ± 0.02
22	2	1	7.5	5000	184 ± 1.8	86.7 ± 3.2	85.6 ± 0.9	-22.8 ± 1.2	0.359 ± 0.01
23	8	1	7.5	5000	186 ± 3.9	85.1 ± 3.3	80.4 ± 0.4	-26.9 ± 0.8	0.364 ± 0.02
24	5	1.75	5	7500	336 ± 4.6	59.4 ± 2.6	55.8 ± 0.6	-30.8 ± 0.2	0.328 ± 0.23
25	-1	1.75	5	7500	495 ± 4.5	45.9 ± 2.9	43.2 ± 1.5	-27.5 ± 0.3	0.197 ± 0.02
26	2	2.5	2.5	5000	652 ± 5.2	45.6 ± 2.4	51.6 ± 1.8	-19.5 ± 0.4	0.459 ± 0.11
27	8	2.5	7.5	5000	264 ± 6.1	78.5 ± 2.5	70.8 ± 1.2	-23.4 ± 0.1	0.294 ± 0.02
28	5	0.25	5	7500	238 ± 5.9	84.2 ± 2.3	64.9 ± 2.4	-29.8 ± 1.1	0.349 ± 0.02
29	8	2.5	7.5	10000	129 ± 3.6	72.3 ± 1.2	69.1 ± 2.9	-22.5 ± 0.2	0.284 ± 0.02
30	8	1	2.5	10000	315 ± 5.9	65.2 ± 2.4	61.3 ± 1.6	-29.1 ± 0.3	0.356 ± 0.12

### 3.3. Time and amplitude of sonication

The greater particle size was seen at 20% amplitude when sonication was done for 5 min, compared to 40% and 50% amplitudes. This might be due to shorter sonication time and lower amplitude. Accordingly, after 2.5 min of sonication at 40% amplitude, particles had shrunk to 200–300 nm, while bigger particles were seen at 20% and 50% amplitude (Table 3). When sonication was done for 2.5 min, the exact amplitude was discovered to be 40%, below which sonication remained incomplete (at 20%) and above which the formulation began to form aggregates (at 50%). The EE, on the other hand, decreased with time when amplitude and sonication duration was increased. Therefore, EMP-SLNs were developed with a 40% amplitude and a sonication period of 2.5 min.

### 3.4. SLN preparation

To create SLNs, researchers used hot homogenization at 5000–10000 rpm at 70 °C and an ultrasonication time of nearly 5–8 min. For this approach to work, an organic miscible solvent (e.g., ethanol) is rapidly diffused into an aqueous solution, causing a significant change in the hydro-organic solvent's dielectric constant and solubility parameter, which intern induces lipid precipitation. Using high-shear mixing and stabilizers in the preparation media, the lipid nanoparticles that comprise the core body of the SLNs are confined to the nanoscale region. The primary benefits of this procedure are its simplicity and the ability to avoid dangerous solvents in the formulation of SLNs reported. Lipids are precipitated in the presence of a stabilizer because ethanol is highly water-soluble and has low interfacial tension in water. This results in the formation of nanoparticles. Homogenization and ultrasonication methods were modified in this investigation to include the ethanolic solution to the liquid phase of the mixture at a temperature of around 50 °C. The particles broke down into smaller sizes when the temperature was higher than the melting point of the lipids. It might be because the organic phase (ethanol) evaporates more quickly, resulting in a lesser inclination for the lipid phase to adhere to the aqueous phase. To further stabilize lipid particles, high temperatures provide surfactants more time to adhere to them.<sup>45</sup> In earlier studies, surfactant concentrations have been shown to influence the synthesis of SLNs, with particle size as the response. There is no significant influence on the particle size as a reaction to other circumstances, such as stirring rate (in a range of 500–2000 g), ethanolic phase addition to the aqueous phase, and so on. As a result, these conditions remained consistent throughout the experiment. Several studies have used this method of comparing the effects of various surfactants.<sup>46–48</sup> Surfactant effects may be evaluated using this method alone, without other interactions. The lipids, EZN, and surfactants were completely soluble in ethanol. Palmitic acid-based SLNs had the highest opalescence features compared to tween 80-based formulations.

### 3.5. Particle size, zeta potential, and polydispersity index

Due to its hydrophobic nature, EZN particle size may be affected by various parameters, including lipid content, surfactant concentration, sonication length, and homogenization speed. We added emulsifier Tween 80 and stabilizer (Poloxamer188) to avoid aggregation of the nanoparticles and SLNs in the formulation to make it pH-sensitive. The findings showed a considerable increase in particle size with increasing lipid content. A particle size analyzer and SEM were used to examine the

**Table 3**

Stabilizer's effect on the creation of SLNs.

Poloxamer 188-Stabilizer Concentration	% EE	Particlesize
0	39.4 ± 2.6	986 ± 26.4
0.5	56.24 ± 3.9	651 ± 6.9
1	79.68 ± 2.5	135 ± 4.2

size and shape of SLNs particles. The particle size, zeta potential, and polydispersity index of EZN-loaded SLNs were analyzed. A direct correlation between particle size and lipid content and an inverse correlation between particle size and surfactant concentration was observed. Sonication duration was also shown to be inversely proportional to particle size. As the surfactant concentration was raised, the particle size decreased due to the increased surface area provided by the high lipid content. Because of the large quantities of macromolecular surfactant chains, the surface was very tight. The stability of nanoparticulate systems is indicated by a zeta potential greater than ±30 mV. There was no evidence of aggregation in the nanoparticles that were created, which is consistent with the results of the Zeta potential measurements. A polydispersity index is a dimensional number that may vary from 0.01 for monodispersed particles up to 0.5–0.8 for highly scattered nanoparticles. Samples with a wide range of sizes tend to have values larger than 0.8. The results showed that the nanoparticle polydispersity index ranged from 0.023 ± 0.03 to 0.642 ± 0.11.

### 3.6. Evaluation of the drug loading and encapsulation efficiency

The results demonstrate that EZN's drug loading capacity is satisfactory, with an EE of 90.6% ± 2.8% and a drug loading capacity of 32.49% ± 1.43% for the optimized formulation F8. Higher lipid content increases drug loading capacity and EE. Owing to the longer time required for lipid precipitation, its entrapment may be limited due to a combination of a low-lying polymer coating and an additional lipid coat. Both EE and drug loading capacity improve gradually with increasing surfactant content. This could be because the medication is floating freely atop the nanoparticle rather than being bound inside entrapped inside the nanoparticles themselves.

### 3.7. Experimental design

In experiment design, the CCD is one response surface model used to reach the goal, reduce variability, and limit or maximize responses to enhance product production or decrease waste. The formulations' results were analyzed to determine the best study design possible. Using DoE VR 12 program, contour plots and desirability plots were produced. Particle size and EE were modeled using a quadratic model. ANOVA was used to identify the variables that significantly impacted the responses. According to the findings (Tables 4 and 5), independent factors such as particle size (nm) and EE (%) had significant effects on the chosen responses, with values ranging from 98.6 ± 2.1 to 431 ± 4.2 nm and 45.6% ± 2.4% to 90.6% ± 2.8%, respectively.

#### 3.7.1. Effect of independent variables on particle size

Solid lipid nanoparticles (SLNs) have a spherical or nearly spherical shape and are made of lipids. Some nanoparticle formulations (such liposomes, which are vesicular structures) share comparable size ranges, which could lead to the term "vesicle" being used. But SLNs aren't hollow like vesicles; they're solid. Like other vesicular structures, such as liposomes or emulsions, SLNs typically have a size that ranges from 100 to 1000 nm. This instance lends itself to the scientifically inaccurate terms "vesicle size" and "nanoparticle size" being used interchangeably.

The following equation may express particle size response (R1) based

**Table 4**

Sonication time and amplitude affect the creation of SLNs.

Sonication time (min)	Amplitude (%)	Particle size (nm)	EE (%)
5	20	459 ± 2.6	69.4 ± 1.2
	40	256 ± 1.6	79.5 ± 0.9
	50	346 ± 3.4	70.2 ± 2.3
8	20	596 ± 4.5	59.4 ± 1.1
	40	346 ± 1.9	62.3 ± 2.4
	50	426 ± 5.3	65.8 ± 1.6

**Table 5**  
ANOVA response for quadratic Modelling.

Parameter	source	DF	Sum of squares	Mean of squares	F Value	p-Value
SIZE	Model	14	3.313E+05	23663.24	18.23	<0.0001
	Residual	15	15376.23	1025.08		
	Lack of fit	10	14658.23	1465.82	1.50	0.3416
	Pure error	5	718.00	143.60		
% EE	Model	14	4423.98	316.00	18.90	<0.0001
	Residual	15	176.98	11.80		
	Lack of fit	10	176.30	17.63	1.22	0.4390
	Pure error	5	0.6750	0.1350		
% CDR	Model	14	3760.00	268.57	22.88	<0.0001
	Residual	15	150.21	10.01		
	Lack of fit	10	148.74	14.87	2.36	0.1779
	Pure error	5	1.47	0.2937		

on the re-gression coefficients computed.

$$\text{Vesicle Size} = +330.00 - 52.52A + 18.65B - 42.73C - 30.93D - 53.15AB - 4.10AC - 12.90AD + 11.77BC - 55.02BD + 62.28CD + 24.31A^2 - 11.07B^2 - 4.19C^2 - 13.44D^2$$

EZN SLNs were generated by varying the independent factors (see Fig. 1). It was determined that the coefficients of determination (R2) and the adjusted R2 for R1 were 0.9556 and 0.9142, respectively, and the unsuitability was deemed barely insignificant. Non-significant ( $p \leq 0.0001$ ). Particle sizes ranged from  $98.6 \pm 2.1$  to  $431 \pm 4.2$  nm in diameter. The particle size was reduced by increasing the sonication time and homogenization speed. Figure 2 shows Particle size response surface plots in three dimensions. The mean particle size of SLNs was significantly reduced by increasing the homogenization speed from 5000 to 10,000 rpm. There was no drastic decrease in particle size when the homogenization speed was increased to 20,000 rpm. For sonication time, the particle size of SLNs reduced as sonication time increased, but additional increases had little impact. Studies have looked at sonication times ranging from 2.5 to 7.5 min. After 2.5 min of sonication, particle size dropped significantly, but an additional sonication duration of 5 min had little impact on particle size. Particle size was unaffected by varying the sonication intensity.

### 3.7.2. Effects of independent variables on the entrapment efficiency

The model was significant according to the quadratic model's F value of 26.78. All terms had a p-value of 0.0001 and were considered important. The adjusted R2 value of 0.9256 showed minor deviations in the experimental model, with a regression coefficient of R2 of 0.9615. In terms of coded factors, the polynomial equation obtained was

$$\text{Entrapment Efficiency} = +60.15 + 3.87A - 2.69B + 3.70C + 3.92D + 5.49AB + 1.23AC - 0.2437AD - 5.32BC + 2.06BD - 8.38CD - 1.90A^2 + 4.64B^2 + 1.20C^2 + 3.37D^2$$

Several different aspects must be considered while creating EZN nanoparticles, as illustrated in Fig. 3. Table 2 shows the findings of drug entrapment in the SLNs formulation. A positive coefficient suggests that the EE was directly related to lipid quantity and the sonication time length. Regarding EE, the term B surfactant concentration has a negative coefficient. The lipid-polymer interaction was studied. Figure 3 depicts each component's influence on the sample's percent EE.

### 3.7.3. Effects of independent variables on cumulative drug release

CDR as a percentage may be expressed as follows in the following way:

$$\text{Cumulative Drug Release} = +55.28 + 3.64A + 0.1208B + 4.77C + 2.63D + 4.86AB - 1.82AC - 0.1812AD - 6.68BC + 1.33BD - 5.42CD - 0.1656A^2 + 3.07B^2 + 2.62C^2 + 5.45D^2$$

Table 6 shows that the model has a substantial F value of 26.82. A good match was established with a correlation value of 0.9897. No significant discrepancies were found between the calculated R2 value of 0.9257 and the expected R2. The precision of 18.1498 (>4) suggested that the signal was sufficient.

In formulations F1–F30, the % CDR ranged from  $43.2\% \pm 1.5\%$  to  $89.2\% \pm 3.6\%$  (Table 2; Fig. 3). According to Eq. (3), the quantity of surfactant and stabilizer was the most significant factor in the percentage CDR, while palmitic acid content was the least significant. The percentage CDR was inversely proportional to the quantity of palmitic acid present. Increasing the quantity of Palmitic acid may lead to larger nanoparticles with less effective surface area for interacting with the release medium, decreasing EZN release. EZN's diffusion route from the organic to the aqueous phase is prolonged when the nanodroplet size rises.<sup>49,50</sup> Drug release properties may improve with increased surfactant concentration due to the surfactant's ability to decrease particle size and increase surface area and drug release.

Particle size and EE were discovered to be affected by homogenization speed, which ranged from 5000 to 10,000 rpm. According to the

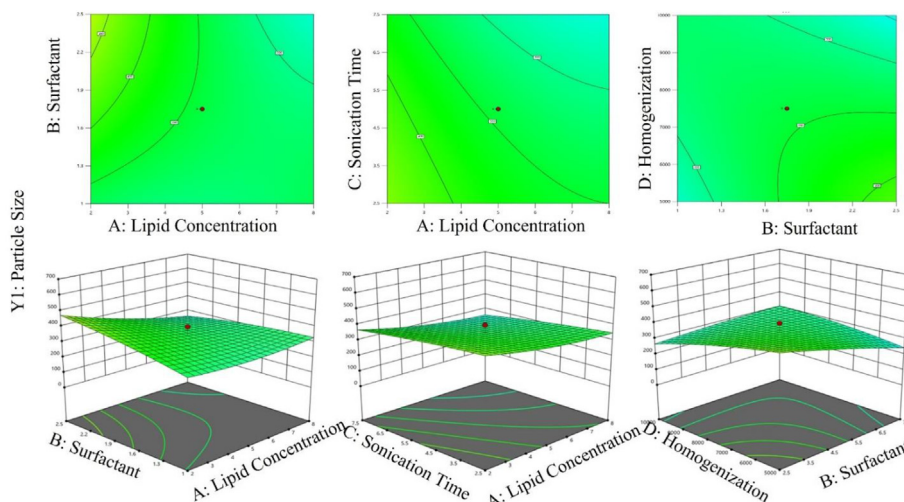


**Fig. 1.** Influence of independent variables on particle size for preparing EZN solid lipid nanoparticles.

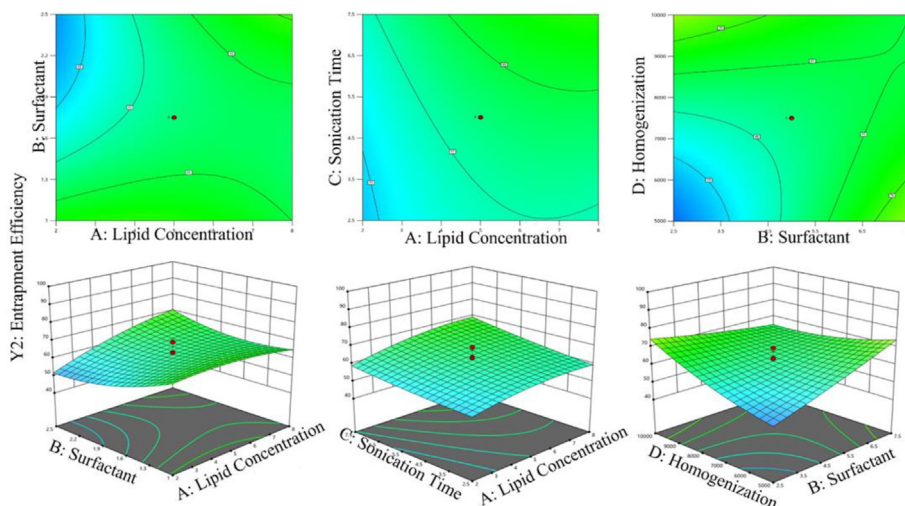


Fig. 2. Influence of independent variables on entrapment efficiency for preparing EZN solid lipid nanoparticles.

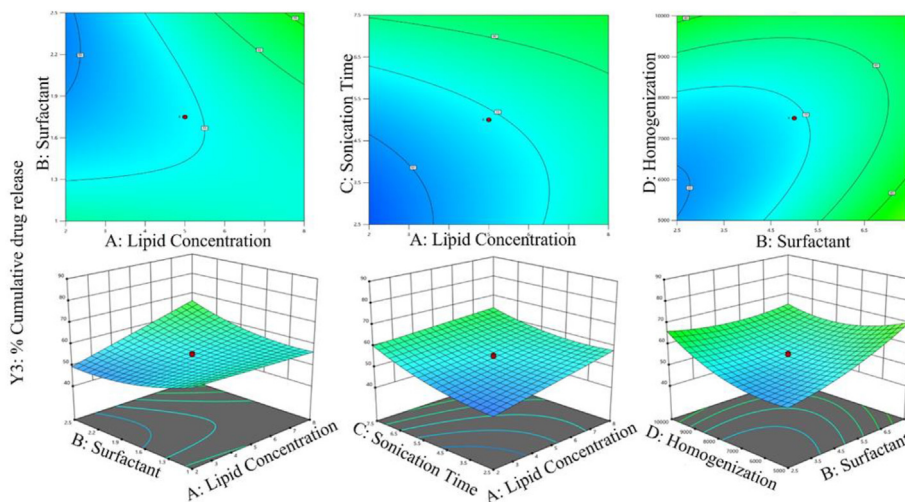


Fig. 3. Cumulative drug release for EZN SLN as influenced by independent factors.

**Table 6**  
EZN Nanoparticle formulation optimization.

Parameters	Actual value	Predicted Value	% Relative Error
R1	98.6 ± 2.1	112.517	13.917
R2	90.6 ± 2.8	88.6458	1.96
R3	89.2 ± 3.6	87.8	1.4

findings, particle size and EE were influenced by homogenization speed. Due to an inability (10,000 rpm), particle size decreased as homogenization speed increased from 5000 to 10,000 revolutions per minute. The shear force exerted on the particles is of such a high intensity that it can overcome the intraparticle forces working within the particles, resulting in a reduction in particle size.<sup>51</sup> The speed of homogenization influences EE, as was found in the current study. EE was enhanced during high-intensity, high-speed homogenization, whereas low-intensity, high-speed processing. Newly produced particles lack a surfactant molecule, resulting in drug diffusion from the lipid matrix of smaller particles with a greater surface area to volume ratio. This resulted in increased drug loss in the SLNs dispersion ([www.sciencedirect.com/science/article/abs/pii/S1773224721002458](http://www.sciencedirect.com/science/article/abs/pii/S1773224721002458)). Because of its lower particle size (98.6 ± 2.1 nm) and greater entrapment effectiveness

(90.6% ± 2.8%) than the other formulations, F8 was chosen because it was the most effective formula and was further investigated. The best formulation has a zeta potential of  $-35.6 \pm 1.2$  mV. Because EZN (which contains a single basic chlorine atom) is oriented on the surface of SLNs, its negative zeta potential might result from this study.<sup>52</sup>

### 3.8. Application of central composite design for formulation optimization

The central composite design was used to make 30 formulations of SLNs, as indicated in Table 2, by choosing four elements at five levels. Dimensions of particles, EE, and drug accumulation were significant dependent variables (responses). DoE VR 12.0.3.0 software was used to develop polynomial equations with coded factors. The most desirable overlay plot from a central point batch was chosen for optimization as advised by the program (Fig. 4). DoE created several possible solutions, and the formulation with the greatest attractiveness score was selected for further optimization. Any answer may have a desirability rating ranging from 0 to 1. If one or more replies fall outside the acceptable range, they are marked with a value of 0 instead of 1. In this scenario, the optimal formulation of nanoparticles desirable is 0.967, and there is a 0.33% possibility of error due to noise. The percent relative error was used to compare the anticipated and actual values of the improved formulation (Table 7). Nano-particles with a relative inaccuracy of less

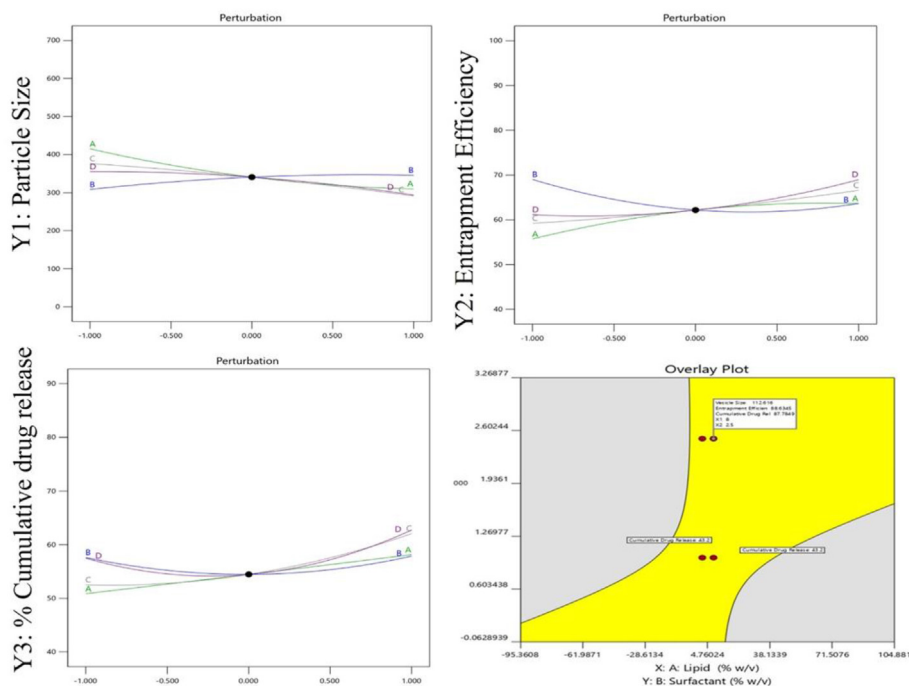


Fig. 4. Perturbation plots and overly plot of optimized EZN SLNs formulation.

Table 7

Data on the pharmacokinetics of EZN suspension and EZN-loaded SLNs.

Pharmacokinetics Parameter	Drug Suspension	Optimized SLNs
C <sub>0</sub> (mcg/mL)	3.585	2.064
K(h <sup>-1</sup> )	0.040	0.010
Dose (mg)	10	10
Vd (mL)	2789.014	4843.385
t <sub>1/2</sub> (hr)	17.324	65.392
Clearance (L/h)	111563.722	51327.627
AUC <sub>0-t</sub> (µg·h/mL)	4.585	2
AUC <sub>t-inf</sub> (µg·h/mL)	5.249	208.540
AUC <sub>Total</sub> (µg·h/mL)	225.915	502.020
MRT <sub>0-t</sub> (h)	15.342	20.649
C <sub>max</sub> (ng/mL)	5.049	5.602
T <sub>max</sub> (h)	11.972	15.857

than 10% indicate that the manufacturing process is stable.<sup>53</sup>

### 3.9. Characterization of solid states

#### 3.9.1. Fourier transform infrared spectroscopy (FT-IR)

FTIR studies were conducted on the drug and its formulation, such as palmitic acid, Tween 80, and poloxamer 188, as shown in Fig. 5. The drug's functional groups have been discovered and mapped. For example, EZN FTIR shows intense bands at 3445.98, 2963.28, 1730.51, 1603, and 1066 cm<sup>-1</sup>, which indicate the presence of quinazoline clusters, aromatic tertiary groups (C-N), carbonyl group stretching (C=O), alkyne stretching, piperidine groups, primary amine stretching (-NH<sub>2</sub>). At 1702 cm<sup>-1</sup> (C=O stretching), 2918 cm<sup>-1</sup> (OH stretching), and 2849 cm<sup>-1</sup>, the FTIR spectra of pal-mitic acid exhibited a prominent peak (CH stretching). There is a long-chain bond visible at 720 cm<sup>-1</sup>, as well as bands for the hydrocarbons CH<sub>2</sub> and CH<sub>3</sub> at 1550 cm<sup>-1</sup> and 1300 cm<sup>-1</sup>. It seems that

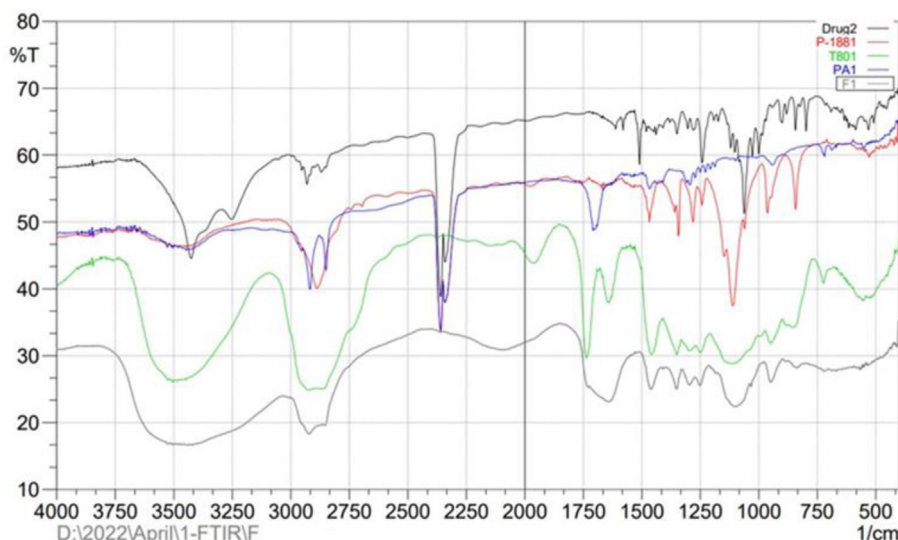


Fig. 5. FTIR spectroscopy studies of the Pure Drug (drug2), Poloxamer 188 (P1881), Tween 80 (T801), Palmitic Acid (PA-1), and optimized formulation (F1).

the intermolecular interactions and molecular reorganization in the SLN structure are connected to the small displacements for  $2918\text{ cm}^{-1}$  (OH stretching) and  $2849\text{ cm}^{-1}$  (CH stretching) in the palmitic acid FTIR spectrum, which reveals almost all absorbances of palmitic acid in SLNs. Surfactants likely are to blame for the additional peaks in the SLN's spectrum. Because of the absence of chemical interactions between the nanocarrier and the drug, the drug's primary structure remains stable throughout the production process. According to the findings, the experiment unaffected EZN's primary peaks ([www.sciencedirect.com/science/article/abs/pii/S1773224721007425](http://www.sciencedirect.com/science/article/abs/pii/S1773224721007425)).

### 3.9.2. DSC

Figure 6 depicts the DSC thermograms of Drug, Palmitic acid, poloxamer 188, and SLNs. The melting of palmitic acid caused the peak to move slightly away from  $64.8\text{ }^{\circ}\text{C}$ , as seen in the graph. There may be a connection between the GMS melting point and this region of stearic acid due to the similarity in melting point. Poloxamer 188 has a temperature peak that is lower than  $55.8\text{ }^{\circ}\text{C}$ . Crystalline nature gave it an endothermic peak at  $151.6\text{ }^{\circ}\text{C}$  for its pure drug melting point. The thermogravimetric analysis confirmed the presence of distinct peaks for each constituent in the physical mixture instance, but the optimized SLNs thermograms showed the presence of lipid and poloxamer peaks and a small broadened drug peak; this could be due to the conversion of a drug from crystallized to amorphous form in SLNs formulations. The FTIR results confirm that the constituent peaks have been slightly displaced, indicating the inter-molecular interaction of the drug and excipients.

### 3.9.3. X-ray diffractogram

The crystallinity and polymorphic nature of SLNs may be determined using X-ray diffractograms. This investigation focused on poloxamer 188, a pure drug, lipids, and optimized SLNs. It is critical to use PXRD to ascertain the polymorphism and crystallinity of API and excipients in solid dosage forms to assure their physical stability. The physical mixtures and diffractograms were compared for polymorphic variations in the PXRD investigation (Fig. 7). At two values, 18.64; 20.18; 25; and 14.52; these results were compared to previously published values, and it was concluded that the crystal form of the drug was crystalline peaks were missing from the SLNs formulation, suggesting that the drug was not crystallized at the time of manufacture. With the SLNs formulation, there was also a reduction in the intensity of pure lipid peaks. This lower intensity proves that the lipid in the SLNs formulation has a decreased crystallinity. This might be because the SLNs formulation was prepared using a solvent evaporation process.

### 3.10. Morphology

SEM, TEM, and AFM were used to determine the optimal formulation's shape and surface morphology. The surfaces of the particles were smooth and spherical, according to the SEM micrograph (Fig. 8A). Most of the optimized SLNs (Fig. 8B) were spheroidal and had a homogeneous distribution, confirming the particle size measurement. According to an AFM study, the SLNs were found to have a spherical form and a particle size of roughly  $100\text{ nm}$  (Fig. 8C). AFM's particle size and dynamic light scattering measurements of particle size are highly connected. SLNs have an average roughness of  $12.035\text{ nm}$ , suggesting that their surfaces are pretty smooth.

### 3.11. Studies on the in vitro release of drug

In the formulation investigations, in vitro release profiles were compared with pure drug solutions (Fig. 9). Analysis and comparison of the release pattern of pure EZN under identical conditions were made with the release of EZN from EZN-SLN. The variation in release pattern is explained as follows. An in vitro drug release test was conducted to evaluate the drug releasing profile of encapsulated EZN SLNs in PBS. This involved simulating the pH conditions of gastric fluid (pH 1.2,  $37\text{ }^{\circ}\text{C}$ ), the first zone of intestinal fluid (pH 6.8,  $37\text{ }^{\circ}\text{C}$ ), and the second intestinal zone fluid and plasma (pH 7.4,  $37\text{ }^{\circ}\text{C}$ ) over a duration of 48 h. As can be shown in Fig. 9, all EZN released 49.3% of their drug in the first 5 h, demonstrating a burst drug release. Additionally, compared to the first 5 h, 95% of the medication contained in SLNs was delivered in a regulated manner after 48 h. In pharmacokinetic testing, the drug's ability to lower blood sugar was lost after 24 h, however EZN SLNs' sustained release profiles demonstrated a longer blood glucose reducing effect that lasted for 48 h. Compared to pure EZN, which had a poor release pattern with a release rate of  $95.64\% \pm 1.81\%$  in 12 h of testing, the EZN-SLNs formulation demonstrated a greater and sustained release of  $91.56\% \pm 2.18\%$  in 48 h. The release of EZN from EZN-SLN exhibited a discernible and consistent pattern of persistence<sup>54</sup>. The rapid release of EZN, which was adsorbed onto the surface of the SLNs, facilitated the observed release behavior. The hydrophobic structure of EZN led to a potent degradation process, resulting in several notable outcomes. These include an extended release duration, enhanced protection against drug release under low pH settings, and controlled release in alkali conditions. Subsequently, the solubilized or dispersed enzyme-zinc nanoparticle (EZN) is gradually released from the inside of the lipid core matrix via diffusion mechanisms, leading to a sustained pattern of release. The

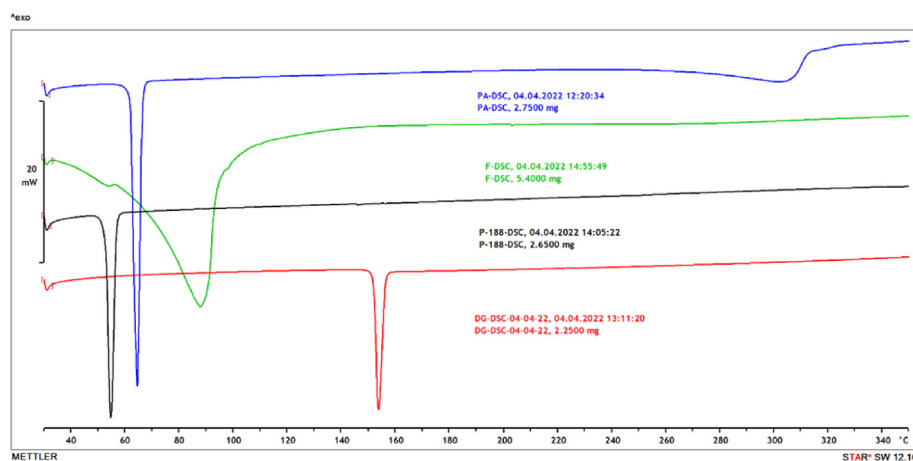


Fig. 6. DSC Thermograms of various excipients and formulations are depicted as an overlay plot. DG: Pure Drug, P188: Poloxamer 188, PA: Palmitic acid, and F: Optimized formula.

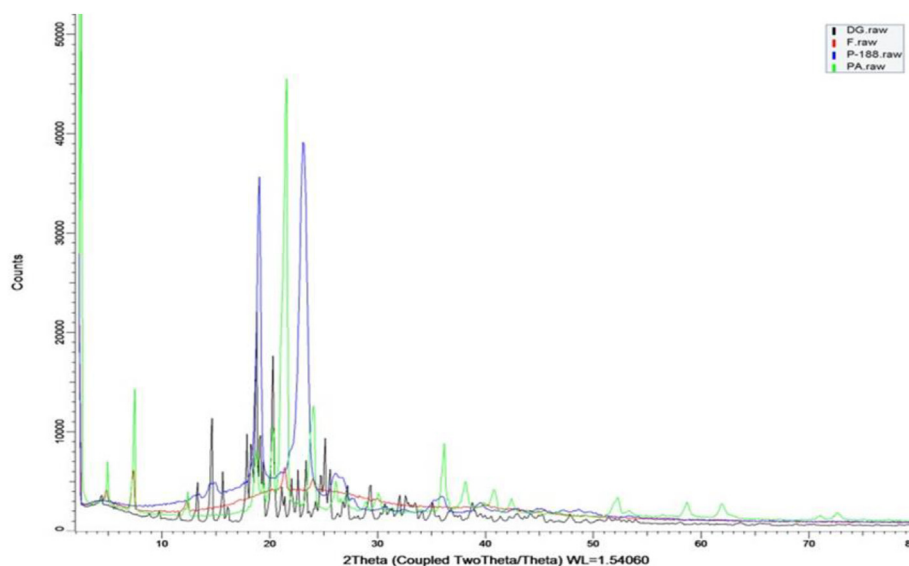


Fig. 7. XRD spectrums of various excipients and formulations are depicted as an overlay plot. DG: Pure Drug, P188: Poloxamer 188, PA: Palmitic acid, and F: Optimized formula.

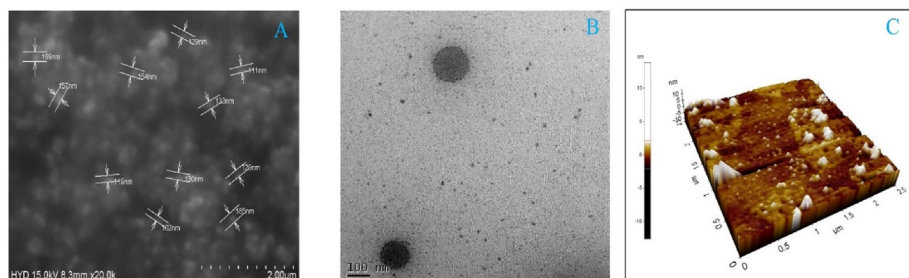


Fig. 8. Investigations on the morphology of an improved formulation A. SEM picture; B. TEM image; C. AFM image.

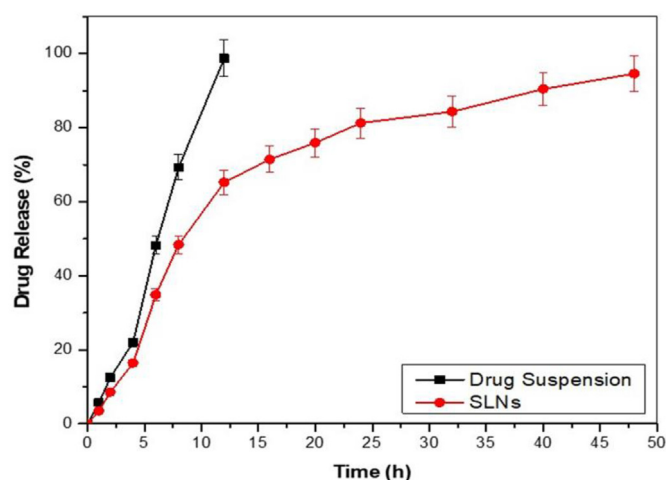


Fig. 9. In vitro release studies of a free drug suspension and optimized SLNs. Values are expressed as Mean  $\pm$  SD. ( $n = 3$ ).

enhanced release of weakly soluble medicines was seen in the EZN-SLNs due to the incorporation of palmitic acid as a solid lipid and tween 80 as a surfactant, which facilitated improved drug release. Various release kinetic models were applied to the release data in order to determine the most appropriate model fit for the investigation. The Korsmeyer-Peppas model was identified as the most suitable release model based on its

highest  $R^2$  value. This method signifies a means of controlled release, achieved through the processes of diffusion and breakdown of a lipid matrix.

The Korsmeyer-Peppas, Higuchi kinetics, zero-order, and first-order models are suitable for analyzing in vitro drug release data. In the optimized batch, the Higuchi model exhibited the highest correlation coefficient ( $R^2 = 0.9889$ ). Diffusion-controlled drug release takes place from a matrix system when the sink conditions are accurately achieved in the release environment. The Higuchi model of release kinetics exhibited a greater degree of linearity compared to the zero-order or first-order kinetics in the ideal formulation. According to the Korsmeyer-Peppas model, it was predicted that the formulation of solid lipid nanoparticles (SLNs) exhibited Fickian diffusion, with a value that was around 0.5.

### 3.12. Pharmacokinetic data

EZN's HPLC validation parameters include the following: Calibration curves were 0.02–10  $\mu\text{g/mL}$  in phosphate buffer; 10–200  $\mu\text{g/mL}$  in rat plasma, linear concentration range, with a retention time of  $5.284 \pm 0.84$  min for the drug. The RSD 2% accuracy and precision for accuracy and precision were attained within and between days. There were two levels of detection: 0.2  $\mu\text{g/mL}$  for LOQ and 0.015  $\mu\text{g/mL}$  for LOD. At doses of 0.2, 0.4, and 2.0  $\mu\text{g/mL}$ , the % entrapment efficiency was  $86.5 \pm 6.57$ ,  $81.39 \pm 7.24$ , and  $92.58 \pm 9.35$  ( $n = 3$ ), respectively. The retention time of the drug was found to be  $2.53 \pm 0.04$  min. Linearity was observed between 5 and 30  $\mu\text{g/mL}$  ( $r^2 = 0.994$ ;  $n = 6$ ). The study showed that the analyte concentration linearly correlates to the peak area. Despite the

precision of the new method, the LOQ was found to be negligible. The accuracy ranged from 99.04 to 102.31% during intraday and interday testing with EZN at concentrations of 5 mcg/mL, moderate (15 µg/mL), and 30 µg/mL(56).

Poor solubility and significant first-pass metabolism restrict EZN's oral bioavailability. EZN has been formulated as SLNs to increase their bioavailability. Male Wistar rats were fed a mixture of suspension and SLNs containing EZN, and the pharmacokinetic parameters were studied. EZN suspension and optimized SLNs were subjected to a graphical analysis of plasma concentration versus time profile (Fig. 10), and their mean pharmacokinetic data is tabulated in Table 8. EZN-loaded SLNs increased the mean plasma concentration in response to the drug and were compared with controls. EZN-loaded SLNs and pure EZN were subjected to a parameter such as AUC 0-total plasma concentrations and found to be 502.020 µg. Hr/mL and 225.91 µg. Hr/mL, respectively. The higher AUC (0–∞) for SLN may be due to lymphatic transport preventing first-pass metabolism.<sup>55</sup> Peyer's patch of the gut, which is essential for lymphatic absorption, may be responsible for the increase in AUC (0–∞) in the study samples. Suspension and SLNs formulation had C<sub>max</sub> values of 5.049 µg/mL and 5.602 µg/mL, respectively. Pure drug suspension had a mean residence time (MRT) of 15.342 h, whereas optimized SLNs had an MRT of 20.649 h. The regulated release of drugs from SLNs may be responsible. To reach maximum plasma concentration ( $T_{max}$ ), the duration was extended from 11.972 h to 15.857 h. SLNs loaded with EZN seem to have a better pharmacokinetic profile than the suspension, according to these findings of the results.

### 3.13. Pharmacodynamic study

Four groups of Wistar rats were used for the pharmacodynamic studies. The rats in groups I and II received normal saline, and were considered normal and diabetic, respectively. Groups III and IV were diabetic rats receiving EZN SLNs and EZN suspension. STZ was used to induce type II diabetes in rats, and blood glucose levels were studied to

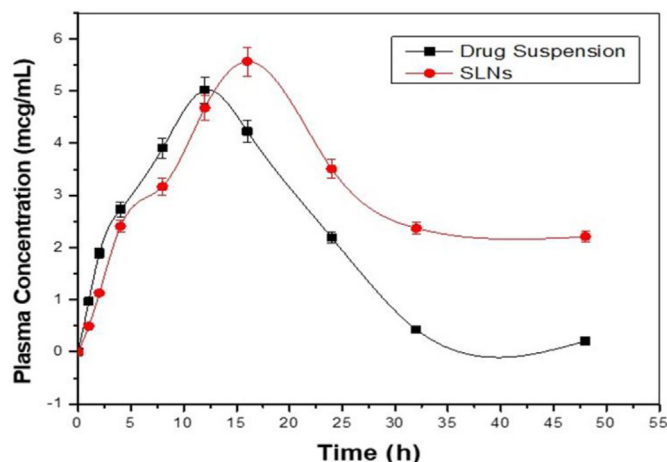


Fig. 10. Pure EZN suspension and EZN-loaded SLN drug level profiles. Mean standard deviation,  $n = 6$ .

Table 8

Stability studies of optimized formulation.

Time	25 °C ± 2 °C/60% ± 5% RH				40 °C ± 2 °C/75% ± 5% RH			
	Appearance	Size	EE	CDR	Appearance	Size	EE	CDR
0	Milky white-colored throughout the study	98.6 ± 2.1	90.6 ± 2.8	89.2 ± 3.6	Milky white-colored throughout the study	98.6 ± 2.1	90.6 ± 2.8	89.2 ± 3.6
30		100.2 ± 3.8	89.5 ± 1.5	87.5 ± 1.2		101.5 ± 3.1	88.3 ± 3.1	86.1 ± 2.5
60		102.8 ± 2.5	88.2 ± 2.4	85.4 ± 2.4		104.6 ± 2.5	85.4 ± 2.1	83.5 ± 2.7
90		104.3 ± 4.1	87.4 ± 3.6	83.2 ± 2.3		105.9 ± 2.1	83.9 ± 2.5	80.5 ± 3.4
180		107.9 ± 3.6	86.9 ± 2.5	800.6 ± 2.1		110.3 ± 2.3	80.8 ± 3.8	76.8 ± 2.6

determine the diabetic condition of rats. Diabetic rats, defined as those with blood sugar levels higher than 200 mg/dL, were used in the study. Groups using EZN suspension or SLNs had blood glucose levels between 155.2 and 212.5 mg/dL and 100.4–220.1 mg/dL, respectively (Fig. 11). EZN's anti-hyperglycemic action was confirmed in both of these groups, which showed substantial ( $p \leq 0.01$ ) decreases in blood sugar levels compared to the diabetic group (Group II). At 4 h, EZN suspension had the most significant effect on blood glucose levels. The promising anti-diabetic activity of EZN-SLNs was enhanced compared to that of the marketed formulation. Accordingly, the increased therapeutic efficacy might be interpreted as acting as a drug substrate for P-gp.

On the other hand, poloxamer 188 and Tween 80 inhibited efflux transporter pump P-gp in EZN-SLNs, leading to higher levels of EZN inflow and bioavailability at 12 h; EZN-SLNs had a significant impact on blood glucose levels. Researchers also found that diabetic rats may be given a lower dosage of EZN-SLNs while monitoring an effective blood glucose level. As a result, EZN-SLNs can increase patient compliance.

### 3.14. Anti-diabetic activity

Figure 12 depicted the impact of a drug suspension and optimized SLNs on blood glucose and insulin levels. Compared to the standard group, diabetic rats had higher blood glucose levels, whereas the SLNs-treated group had a substantial drop in blood glucose levels. When comparing the diabetes group to the control group, it was discovered that the plasma insulin level rise in the treatment group. SLNs were more successful in lowering insulin levels than drug suspensions. These findings show that SLNs were more effective in treating diabetes than EZN suspensions in experimental animal models. Levels of blood glucose (A) and plasma (B) in rats ( $n = 6$  for each group). The graph depicts mean ± SD. \* $p < 0.05$ , \*\* $p < 0.01$ , \*\*\* $p < 0.001$ .

### 3.15. Stability studies

A product's shelf life had to be determined using stability experiments, including raising the temperature and humidity to hasten decomposition. For six months, the improved formulation was kept between 25 °C and 40 °C and 60% and 75% RH and periodically examined for changes in physical appearance, EE, particle size, and drug release by ICH guidelines. According to the results (Table 8), even after six months of stress testing, there was no difference in the appearance of SLNs.

## 4. Conclusions

In conclusion, based on lipid solubility tests, palmitic acid was chosen to prepare SLNs. Stabilizer concentration, frequency, and period of sonication were determined by conducting pilot experiments. Preparation of SLNs using the CCD design in which independent variables such as lipid content, sonication time, homogenization speed, and surfactant concentration have a response on dependent variables cumulatively drug release, EE, and particle size. It was found that the optimized formulation prepared by CCD had less particle size with greater EE and cumulative drug release near-est to the predicted values (98.6% ± 2.1%, 90.6% ± 2.8%, and 89.2% ± 3.6%, respectively). The invitro drug release showed an initial burst release followed by sustain release of the formulated EZN

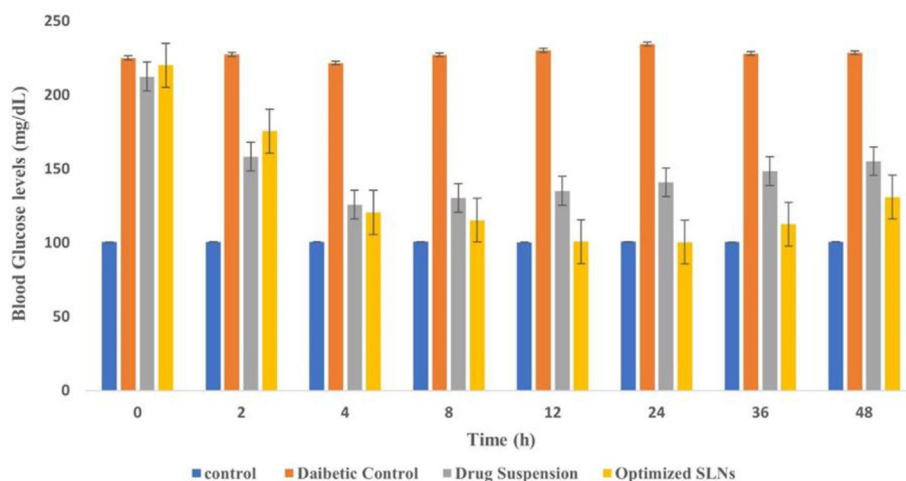


Fig. 11. Concentration (mg/dL) of EZN (EZN-SLNs) in blood glucose (mg/dL) (pharmacodynamic study).

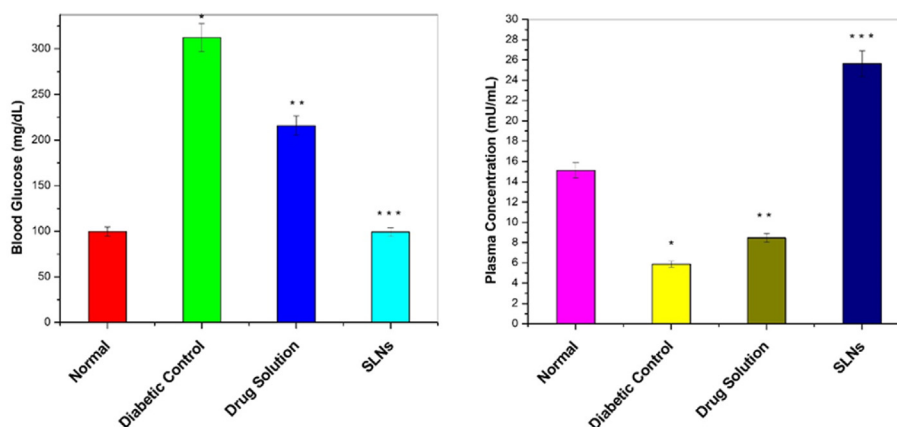


Fig. 12. Blood glucose and plasma levels in treated rats after induction of STZ.

SLNs. In the formulation, the morphological findings indicated that the particles were spherical and evenly distributed. According to the DSC studies, the drug was shifted from crystallization to amorphous nature. Improved pharmacokinetics and better anti-diabetic effectiveness were demonstrated and confirmed by in vivo experiments comparing it to an optimized formulation. EZN oral administration through the SLNs route may be an opted for treating DM. In turn, the prepared SLNs showed higher bioavailability and better compliance over glycemic control in experimental animals.

#### CRediT authorship contribution statement

**Ananda Kumar Chettupalli:** Investigation, Formal analysis. **Aziz Unnisa:** Writing – original draft, Project administration, Funding acquisition. **Himabindu Peddapalli:** Validation. **Rajendra Kumar Jadi:** Data curation, Conceptualization. **Kachupally Anusha:** Supervision. **Padmanabha Rao Amarachinta:** Resources, Methodology.

#### Informed consent statement

Not relevant.

#### Institutional review Board statement

The IAEC of the School of Pharmacy, Nalanda College of Pharmacy, Hyderabad, Telangana (reference number NCP/IAEC/08–22/013) authorized all animal research.

#### Conflicts of interest

There are no conflicts of interest among the writers. The funders had no part in the design of the research; in the collection, analysis, or interpretation of data; in the writing of the paper; or in the decision to publish the findings.

#### Acknowledgements

The Authors are thankful to the Deans of their respective colleges for their support in carrying out this research.

#### References

- Inzucchi SE, Bergenstal RM, Buse JB, et al. Management of Hyperglycemia in Type 2 Diabetes, 2015: a Patient-Centered Approach: update to a position statement of the American diabetes association and the European association for the study of diabetes. *Diabetes Care*. 2015;38(1):140–149.
- Pawlak R. Vegetarian diets in the prevention and management of diabetes and its complications. *Diabetes Spectr*. 2017;30(2):82–88.
- Sepehri Z, Kiani Z, Afshari M, Kohan F, Dalvand A, Ghavami S. Inflammation and type 2 diabetes: an updated systematic review. *Immunol Lett*. 2017;192:97–103.
- Nawaz MS, Shah KU, Khan TM, et al. Evaluation of current trends and recent development in insulin therapy for management of diabetes mellitus. *Diabetes Metab Syndr Clin Res Rev*. 2017;11:S833–S839.
- Grube A, Gerlitzki C, Brendel M. Dissolution or disintegration–substitution of dissolution by disintegration testing for a fixed dose combination product. *Drug Dev Ind Pharm*. 2019;45(1):130–138.
- Acharya T, Deedwania P. Cardiovascular outcome trials of the newer anti-diabetic medications. *Prog Cardiovasc Dis*. 2019;62(4):342–348.

7. Hedrington MS, Davis SN. The role of empagliflozin in the management of type 2 diabetes by patient profile. *Therapeut Clin Risk Manag.* 2015;11:739–749.
8. Rodbard HW, Blonde L, Braithwaite SS, et al. American association of clinical endocrinologists medical guidelines for clinical practice for the management of diabetes mellitus. *Endocr Pract.* 2007;13(SUPPL. 1):1–68.
9. Levine MJ. Empagliflozin for type 2 diabetes mellitus: an overview of phase 3 clinical trials. *Curr Diabetes Rev.* 2016;13(4).
10. Frampton JE. Empagliflozin: a review in type 2 diabetes. *Drugs.* 2018;78(10):1037–1048.
11. Yoon G, Park JW, Yoon IS. Solid lipid nanoparticles (SLNs) and nanostructured lipid carriers (NLCs): recent advances in drug delivery. *J Pharm Investig.* 2013;43(5):353–362.
12. Makwana V, Jain R, Patel K, Nivsarkar M, Joshi A. Solid lipid nanoparticles (SLN) of Efavirenz as lymph targeting drug delivery system: elucidation of mechanism of uptake using chylomicron flow blocking approach. *Int J Pharm.* 2015;495(1):439–446.
13. Mishra V, Bansal KK, Verma A, et al. Solid lipid nanoparticles: emerging colloidal nano drug delivery systems. *Pharmaceutics.* 2018;10(4).
14. Vanti G, Muti L, D'ambrosio M, et al. Nanostructured lipid carriers can enhance oral absorption of khellin, a natural pleiotropic molecule. *Molecules.* 2021;26(24):7657.
15. Stella V, Peira E, Dianzani C, et al. Development and characterization of solid lipid nanoparticles loaded with a highly active doxorubicin derivative. *Nanomaterials.* 2018;8(2).
16. Trevaskis NL, Kaminskas LM, Porter CJH. From sewer to saviour—targeting the lymphatic system to promote drug exposure and activity. *Nat Rev Drug Discov.* 2015;14:781–803.
17. Porter CJH, Trevaskis NL, Charman WN. Lipids and lipid-based formulations: optimizing the oral delivery of lipophilic drugs. *Nat Rev Drug Discov.* 2007;6:231–248.
18. Soni K, Rizwanullah M, Kohli K. Development and optimization of sulforaphane-loaded nanostructured lipid carriers by the Box-Behnken design for improved oral efficacy against cancer: in vitro, ex vivo and in vivo assessments. *Artif Cells, Nanomedicine Biotechnol.* 2018;46(sup1):15–31.
19. Harde H, Das M, Jain S. Solid lipid nanoparticles: an oral bioavailability enhancer vehicle. *Expet Opin Drug Deliv.* 2011;8(11):1407–1424.
20. Miller DB, Spence JD. Clinical pharmacokinetics of fibric acid derivatives (Fibrates). *Clin Pharmacokinet.* 1998;34(2):155–162.
21. Ganesan P, Ramalingam P, Karthivashan G, Ko YT, Choi DK. Recent developments in solid lipid nanoparticle and surface-modified solid lipid nanoparticle delivery systems for oral delivery of phyto-bioactive compounds in various chronic diseases. *Int J Nanomed.* 2018;13:1569–1583.
22. Doktorovova S, Souto EB, Silva AM. Hansen solubility parameters (HSP) for prescreening formulation of solid lipid nanoparticles (SLN): in vitro testing of curcumin-loaded SLN in MCF-7 and BT-474 cell lines. *Pharmaceut Dev Technol.* 2018;23(1):96–105.
23. Müller RH, Mäder K, Gohla S. Solid lipid nanoparticles (SLN) for controlled drug delivery - a review of the state of the art. *Eur J Pharm Biopharm.* 2000;50(1):161–177.
24. Zur Mühlen A, Schwarz C, Mehnert W. Solid lipid nanoparticles (SLN) for controlled drug delivery - drug release and release mechanism. *Eur J Pharm Biopharm.* 1998;45(2).
25. Beg S, Rahman M, Kohli K. Quality-by-design approach as a systematic tool for the development of nanopharmaceutical products. *Drug Discov Today.* 2019;24(3):717–725.
26. Unnisa A, Chettupalli AK, Hagbani T AI, et al. Development of dapagliflozin solid lipid nanoparticles as a novel carrier for oral delivery: statistical design, optimization, in-vitro and in-vivo characterization, and evaluation. *Pharmaceutics.* 2022;15(5).
27. Mujeli M, Hussain SA, Ismail MHS, Biak DRA, Jami MS. Screening of electrocoagulation process parameters for treated palm oil mill effluent using minimum-runs resolution IV design. *Int J Environ Sci Technol.* 2019;16(2):811–820.
28. Gidwani B, Vyas A. Preparation, characterization, and optimization of alretamine-loaded solid lipid nanoparticles using Box-Behnken design and response surface methodology. *Artif Cells, Nanomedicine Biotechnol.* 2016;44(2):571–580.
29. Cirri M, Bragagni M, Mennini N, Mura P. Development of a new delivery system consisting in “drug - in cyclodextrin - in nanostructured lipid carriers” for ketoprofen topical delivery. *Eur J Pharm Biopharm.* 2012;80(1):46–53.
30. Shah H, Patel R. Statistical modeling of zaltoprofen loaded biopolymeric nanoparticles: characterization and anti-inflammatory activity of nanoparticles loaded gel. *Int J Pharm Investig.* 2015;5(1):20.
31. Behbahani ES, Ghaedi M, Abbaspour M, Rostamizadeh K. Optimization and characterization of ultrasound assisted preparation of curcumin-loaded solid lipid nanoparticles: application of central composite design, thermal analysis and X-ray diffraction techniques. *Ultrason Sonochem.* 2017;38:271–280.
32. Khalil HE, Alqahtani NK, Darrag HM, et al. Date palm extract (*Phoenix dactylifera*) PEGylated nanoemulsion: development, optimization and cytotoxicity evaluation. *Plants.* 2021;10(4).
33. Zhang L, Hao W, Xu L, et al. A pH-sensitive methenamine mandelate-loaded nanoparticle induces DNA damage and apoptosis of cancer cells. *Acta Biomater.* 2017;62:246–256.
34. Sahle FF, Balzus B, Gerecke C, Kleuser B, Bodmeier R. Formulation and in vitro evaluation of polymeric enteric nanoparticles as dermal carriers with pH-dependent targeting potential. *Eur J Pharmaceut Sci.* 2016;92:98–109.
35. Padhye SG, Nagarsenker MS. Simvastatin solid lipid nanoparticles for oral delivery: formulation development and in vivo evaluation. *Indian J Pharmaceut Sci.* 2013;75(5):591–598.
36. Khaira R, Sharma J, Saini V. Development and characterization of nanoparticles for the delivery of gemcitabine hydrochloride. *Sci World J.* 2014;2014.
37. Priyanka K, Sahu PL, Singh S. Optimization of processing parameters for the development of *Ficus religiosa* L. extract loaded solid lipid nanoparticles using central composite design and evaluation of antidiabetic efficacy. *J Drug Deliv Sci Technol.* 2018;43:94–102.
38. Sharma JB, Bhatt S, Saini V, Kumar M. Pharmacokinetics and pharmacodynamics of curcumin-loaded solid lipid nanoparticles in the management of streptozotocin-induced diabetes mellitus: application of central composite design. *Assay Drug Dev Technol.* 2021;19(4):262–279.
39. Wójcik-Pastuszka D, Krzak J, Macikowski B, Berkowski R, Osiński B, Musiał W. Evaluation of the release kinetics of a pharmacologically active substance from model intra-articular implants replacing the cruciate ligaments of the knee. *Materials.* 2019;12(8).
40. Chadha R, Bhandari S. Drug-excipient compatibility screening—Role of thermoanalytical and spectroscopic techniques. *J Pharmaceut Biomed Anal.* 2014;87:82–97.
41. Prisilla DH, Balamurugan R, Shah HR. Antidiabetic activity of methanol extract of *Acorus calamus* in STZ induced diabetic rats. *Asian Pac J Trop Biomed.* 2012;2(2 suppl L).
42. Qia I. Stability testing guidelines: stability testing of new drug substances and products. [Internet]. *ICH Steering Committee*; 2003, 2003. p. 1–24. Available from: [www.ema.europa.eu/en/ich-q1a-r2-stability-testing-new-drug-substances-drug-prod-ucts-scientific-guideline](http://www.ema.europa.eu/en/ich-q1a-r2-stability-testing-new-drug-substances-drug-prod-ucts-scientific-guideline).
43. Chalikwar SS, Belgamwar VS, Talele VR, Surana SJ, Patil MU. Formulation and evaluation of Nimodipine-loaded solid lipid nanoparticles delivered via lymphatic transport system. *Colloids Surfaces B Biointerfaces.* 2012;97:109–116.
44. Aji Alex MR, Chacko AJ, Jose S, Souto EB. Lopinavir loaded solid lipid nanoparticles (SLN) for intestinal lymphatic targeting. *Eur J Pharmaceut Sci.* 2011;42(1–2):11–18.
45. Helgason T, Awad TS, Kristbergsson K, McClements DJ, Weiss J. Effect of surfactant surface coverage on formation of solid lipid nanoparticles (SLN). *J Colloid Interface Sci.* 2009;334(1):75–81.
46. Kovacevic A, Savic S, Vuleta G, Müller RH, Keck CM. Polyhydroxy surfactants for the formulation of lipid nanoparticles (SLN and NLC): effects on size, physical stability and particle matrix structure. *Int J Pharm.* 2011;406(1–2):163–172.
47. Olbrich C, Müller RH. Enzymatic degradation of SLN-effect of surfactant and surfactant mixtures. *Int J Pharm.* 1999;180(1):31–39.
48. Schöler N, Olbrich C, Tabatt K, Müller RH, Hahn H, Liesenfeld O. Surfactant, but not the size of solid lipid nanoparticles (SLN) influences viability and cytokine production of macrophages. *Int J Pharm.* 2001;221(1–2):57–67.
49. Lalani J, Patil S, Kolate A, Lalani R, Misra A. Protein-functionalized PLGA nanoparticles of lamotrigine for neuropathic pain management. *AAPS PharmSciTech.* 2015;16(2):413–427.
50. Manoochehri S, Darvishi B, Kamalinia G, et al. Surface modification of PLGA nanoparticles via human serum albumin conjugation for controlled delivery of docetaxel. *DARU, J Pharm Sci.* 2013;21(1).
51. Quintanar-Guerrero D, Fessi H, Allémann E, Doelker E. Influence of stabilizing agents and preparative variables on the formation of poly(D,L-lactic acid) nanoparticles by an emulsification-diffusion technique. *Int J Pharm.* 1996;143(2):133–141.
52. Bakshi V, Amarachinta PR, Chettupalli AK. Design, development and optimization of solid lipid nanoparticles of rizatriptan for intranasal delivery: invitro & invivo assessment. *Mater Today Proc.* 2022;66:2342–2357.
53. Amarachinta PR, Sharma G, Samed N, Chettupalli AK, Alle M, Kim JC. Central composite design for the development of carvedilol-loaded transdermal ethosomal hydrogel for extended and enhanced anti-hypertensive effect. *J Nanobiotechnology.* 2021;19(1).
54. Anchi P, Khurana A, Swain D, Samanthula G, Godugu C. Dramatic improvement in pharmacokinetic and pharmacodynamic effects of sustain release curcumin microparticles demonstrated in experimental type 1 diabetes model. *Eur J Pharmaceut Sci.* 2019;130:200–214.
55. Kumar VV, Chandrasekar D, Ramakrishna S, Kishan V, Rao YM, Diwan PV. Development and evaluation of nitrendipine loaded solid lipid nanoparticles: influence of wax and glyceride lipids on plasma pharmacokinetics. *Int J Pharm.* 2007;335(1–2):167–175.